Published in final edited form as:
Science. 2011 February 18; 331(6019): 916–920. doi:10.1126/science.1195774.

Distinct properties of the XY pseudoautosomal region crucial for male meiosis

Liisa Kauppi[1], **Marco Barchi**[2,3], **Frédéric Baudat**[2,*], **Peter J. Romanienko**[2], **Scott Keeney**[1,4], and **Maria Jasin**[2]

[1] Molecular Biology, Memorial Sloan-Kettering Cancer Center, New York, NY 10065, USA

[2] Developmental Biology Programs, Memorial Sloan-Kettering Cancer Center, New York, NY 10065, USA

[3] Department of Public Health and Cell Biology, Section of Anatomy, University of Rome Tor Vergata, 00133 Rome, Italy

[4] Howard Hughes Medical Institute, Memorial Sloan-Kettering Cancer Center, New York, NY 10065, USA

Abstract

Meiosis requires that each chromosome finds its homologous partner and undergoes at least one crossover. X-Y chromosome segregation hinges on efficient crossing-over in a very small region of homology, the pseudoautosomal region (PAR). We find that mouse PAR DNA occupies unusually long chromosome axes, potentially as shorter chromatin loops, predicted to promote double-strand break (DSB) formation. Most PARs show delayed appearance of RAD51/DMC1 foci, which mark DSB ends, and all PARs undergo delayed DSB-mediated homologous pairing. Analysis of *Spo11β* isoform-specific transgenic mice revealed that late RAD51/DMC1 foci on the PAR are genetically distinct from early PAR foci and global foci, and that late PAR foci promote efficient X-Y pairing, recombination and male fertility. Our findings uncover specific mechanisms that surmount the unique challenges of X-Y recombination.

Meiotic recombination, initiated by programmed DSBs, promotes homologous chromosome (homolog) pairing during prophase I (1). A subset of DSBs matures into crossovers that physically connect homologs so they orient properly on the first meiotic spindle. Because sex chromosome recombination and pairing are restricted to the PAR (2), at least one DSB must form within this small region and the homologous PAR must be located and engaged in recombination leading to a crossover. Accordingly, the PAR in males exhibits high crossover frequency (2, 3) but sex chromosomes also mis-segregate more frequently than autosomes (4). Nevertheless, X-Y non-disjunction is rare, suggesting the existence of mechanisms that ensure successful X-Y recombination.

X-Y pairing is more challenging than autosomal pairing, as it cannot be mediated by multiple DNA interactions along the length of the chromosomes. We used fluorescence in situ hybridization (FISH) (5) to compare timing of meiotic X-Y and autosomal pairing in mice (Fig. 1). At leptonema when DSBs begin to form and only short chromosome axis segments are present, PAR and autosomal FISH probes were mostly unpaired. By early/mid-zygonema, when axes elongate and homologs become juxtaposed, distal ends of Chr 18 and

Corresponding authors: MJ: Phone (212) 639-7438; FAX: (212) 717-3317; m-jasin@ski.mskcc.org. SK: Phone (212) 639-5182; FAX: (212) 717-3627; s-keeney@ski.mskcc.org.
*Present address: Institute of Human Genetics, CNRS, Montpellier, France

19 were paired in ~50% of nuclei; by late zygonema, these regions were paired in nearly all nuclei (Fig. 1B, fig. S1). In contrast, the X and Y PARs were rarely paired before pachynema (Fig. 1B), hence X-Y pairing is delayed compared to autosomes.

DSBs precede and are required for efficient homolog pairing in mouse meiosis (6, 7). Nucleus-wide ("global") foci of DSB markers RAD51/DMC1 peak in number at early/mid-zygonema (Fig. 2A, (8, 9)). Because stable X-Y pairing occurs late, we asked whether PAR DSB kinetics are also delayed (Fig. 2B, fig. S2). More than half of cells had no RAD51/DMC1 focus in the PAR before late zygonema (Figs. 2B–C, fig. S2*iii*), distinct from global patterns. Only when global foci were already declining did the majority of cells (~70%) display PAR foci (Fig. 2C, fig. S2*i*). We interpret lack of PAR foci to indicate that DSBs have not yet formed. Thus we propose that PAR DSB formation and/or turnover are under distinct temporal control. We cannot exclude the alternative possibility that PAR DSBs have formed but are cytologically undetectable, for example because RAD51/DMC1 have not yet been loaded onto DSB ends, or because foci have already turned over (fig. S3). In either case, DSB dynamics/processing differs on the PAR.

Most sites marked by PAR RAD51/DMC1 foci appeared incapable of mediating stable pairing prior to early pachynema (~70% of late zygotene nuclei had foci, but <20% showed PAR pairing, Figs. 1B, 2C). The number of PAR foci per cell also increased over time. In leptonema and early/mid-zygonema, most cells with a PAR RAD51/DMC1 focus had only one (typically on X), whereas by late zygonema, two PAR foci were often present (both X and Y, Fig. 2C, fig. S2). Foci on both PARs could represent two independent DSBs. If so, then having more than one X-Y recombination interaction may stabilize pairing, similar to multiple interactions which stabilize pairing of autosomes (10). Alternatively, foci on both PARs could represent the two, separated ends of a single DSB (11, 12), with one focus marking the broken PAR and the second focus marking the other PAR (fig. S3A). In this "ends-apart" model, nuclei that have two PAR foci are those in which the X and Y PARs have successfully engaged each other. However, we found that most such nuclei showed no evidence of a preferential X-Y spatial relationship (fig. S3B), and most PAR pairing occurred abruptly at the zygonema-to-pachynema transition, i.e., after the stage when many cells displayed two PAR foci (compare Figs. 1B, 2C). Sex body formation (13) may facilitate this sudden completion of X-Y pairing by providing homology-independent X-Y proximity that simplifies the homology search.

The haploid mouse genome averages <1 DSB/10 Mb (Fig. 2A), whereas the <1 Mb PAR (14) undergoes 1–2 DSBs (Fig. 2C), 10–20-fold higher than genome average. We speculated that distinct higher order chromosome structure could render the PAR more conducive to DSB formation. Meiotic recombination is proposed to occur within DNA segments residing in chromatin loops that become transiently tethered to chromosome axes (15). Loop density per μm of axis is constant (16), producing an inverse relationship between loop size and axis length (17). DNA arranged into smaller loops may have higher DSB potential (Fig. 2D) (18); indeed, autosomal crossover frequency in male mice correlates with axis length (19). We found that PAR axes were disproportionately long relative to DNA length, incorporating ~1 Mb/μm of axis (Table 1A). At distal ends of Chr 18 and 19 (regions with relatively frequent crossing-over (19)), DNA content was 10–13 Mb/μm and correlated well with axis length, i.e., the distal ~10% of DNA occupied ~10% total axis length (Table 1A). The ≥10-fold difference between PAR and autosome axes is of the magnitude expected for a region that experiences >10-fold more DSBs. Axes of non-PAR portions of the X and Y had a more autosome-like DNA content (≥14 Mb/μm, fig. S4).

Long PAR axes predict short chromatin loops. As a proxy for loop size we measured FISH signal extension from axes for probes in the PAR and autosomal subtelomeric regions (Fig.

2E, Table 1B). PAR FISH signals were substantially more compact at all stages (~3–7-fold less extended), consistent with smaller loops. Thus, chromosome structure could be one factor that facilitates high-frequency DSB formation in the PAR.

The distinct temporal and structural features outlined above raised the possibility that mechanisms ensuring efficient PAR recombination and pairing may be under different genetic control from autosomes. Characterization of a variant of SPO11, the evolutionarily conserved meiotic DSB catalyst (1), validated this hypothesis (Fig. 3). Two major mRNA splicing isoforms in mice and humans are *Spo11α* and *Spo11β* (7, 20–22), (Fig. 3A*i*, fig. S5). *Spo11β* is expressed early in meiosis, when most DSBs are formed (Fig. 2A), whereas *Spo11α* is expressed later (7, 20, 23) (Fig. 3A*ii*, fig. S6A). Thus, SPO11β is likely responsible for most DSB formation.

We generated transgenic mice expressing $Spo11\beta_B$ cDNA (fig. S5) from a meiosis-specific promoter (24) (fig. S6B). *Tg(Xmr-*$Spo11\beta_B$) transcript expression overlapped with *Spo11β* mRNA appearance in wild type (Fig. 3A*ii*, figs. S6A, S6C). In testis extracts of $Spo11^{-/-}$ *Tg(Xmr-*$Spo11\beta_B)^{+/+}$ (hereafter, "*Spo11β*-only") mice, $SPO11\beta_B$ protein approximated the total level of SPO11 in wild type (Fig. 3A*iii*). The transgene did not cause obvious meiotic phenotypes in mice heterozygous at the endogenous *Spo11* locus (i.e., $Spo11^{+/-}$ *Tg(Xmr-*$Spo11\beta_B)^{+/+}$), and these mice were used as controls. The profound meiotic defects of $Spo11^{-/-}$ mice (no recombination, failure of homolog pairing and synapsis, infertility (6, 7, 25)) were mostly rescued by *Tg(Xmr-*$Spo11\beta_B$) in both sexes: autosomal homologous pairing, synapsis and MLH1 focus formation (a crossover marker) appeared normal (Fig. 3B*i*, fig. S7A). Moreover, ovaries of *Spo11β*-only mice contained abundant primordial follicles (Fig. S7B) and *Spo11β*-only females were fully fertile with normal litter sizes. Thus $SPO11\beta_B$ supports autosomal crossing-over, pairing and synapsis, and (in females) full meiotic progression and accurate chromosome segregation. Male meiosis was not fully rescued, however. Although sex bodies formed (fig. S7C), the X and Y failed to pair and synapse in ~70% of spermatocytes (Fig. 3B). *Spo11β*-only testis sections showed numerous apoptotic metaphase I cells (Fig. 3C), many with a lagging chromosome (Fig. 3C, **inset**), consistent with spindle checkpoint-induced apoptosis (9, 13, 26, 27) triggered by the failure of non-recombinant X and Y to orient properly on the metaphase I spindle. Few post-meiotic cells were formed and testis sizes were reduced (Fig. 3C, fig. S7D–E), and while some *Spo11β*-only males produced offspring, most were infertile.

Nucleus-wide numbers and timing of RAD51/DMC1 foci were indistinguishable between *Spo11β*-only and control males (Fig. 3D, fig. S7F) indicating that the X-Y pairing defect cannot be attributed to reduced global DSB levels (Fig. 3E). Similarly, the frequency of PAR RAD51/DMC1 foci in leptonema was not affected. In contrast, the percentage of late zygotene nuclei with a PAR focus was reduced in *Spo11β*-only males, consistent with a defect in a late-forming DSB population (PAR-specific, or possibly including a small subset of autosomal DSBs). ~70% of late zygotene nuclei lacked PAR foci (Fig. 3E), similar to the percentage of cells with X-Y pairing failure (Fig. 3B*iii*). Thus the few PAR foci that form early in both wild-type and *Spo11β*-only males seem to persist until late zygonema (fig. S4 discussion), at which time recombination-mediated X-Y pairing occurs. We propose that a lack of late PAR DSBs is the cause of infertility in *Spo11β*-only males. In females, two fully homologous X chromosomes make PAR recombination dispensable.

Spo11α is the only splice variant missing from *Spo11β*-only mice that is known to be developmentally regulated, and its expression in wild type correlates with the timing of late PAR DSBs as inferred from the appearance of RAD51/DMC1 foci. It is thus possible that SPO11α, by itself or in combination with SPO11β, is needed for DSB formation in late zygonema. In this scenario, late-forming PAR DSBs are genetically separable both from

global DSBs and from early-forming PAR DSBs, and that the surge of late-forming PAR DSBs is crucial for efficient X-Y pairing and fertility. PAR recombination occasionally fails in humans, as evidenced by paternally inherited sex chromosome aneuploidies (e.g. Klinefelter or Turner syndromes (28)). Because *Spo11* isoforms are conserved, we speculate that variation in *Spo11* splicing patterns may be a human X-Y non-disjunction susceptibility trait.

Supplementary Material

Refer to Web version on PubMed Central for supplementary material.

Acknowledgments

This work was supported by NIH grant R01 HD040916 (M.J., S.K); AIRC (MFAG grant 4765), MIUR, the Lalor Foundation, and the AICF (M.B.); and the Charles H. Revson Foundation (F.B.). We thank Margaret Leversha (MSKCC), Philippe Bois (Scripps Florida), and Katia Manova (MSKCC) for valuable advice and protocols. We are grateful to Keeney and Jasin lab members, especially Ignasi Roig, Esther de Boer and Francesca Cole, and to Neil Hunter (UC Davis) for insightful comments.

References and Notes

1. Cole F, Keeney S, Jasin M. Genes Dev. 2010; 24:1201. [PubMed: 20551169]
2. Rouyer F, et al. Nature. 1986; 319:291. [PubMed: 3941746]
3. Soriano P, et al. Proc Natl Acad Sci U S A. 1987; 84:7218. [PubMed: 3478692]
4. Shi Q, et al. Am J Med Genet. 2001; 99:34. [PubMed: 11170091]
5. Materials and methods are available as supporting material on *Science* Online.
6. Baudat F, Manova K, Yuen JP, Jasin M, Keeney S. Mol Cell. 2000; 6:989. [PubMed: 11106739]
7. Romanienko PJ, Camerini-Otero RD. Mol Cell. 2000; 6:975. [PubMed: 11106738]
8. Ding X, et al. Dev Cell. 2007; 12:863. [PubMed: 17543860]
9. Barchi M, et al. PLoS Genet. 2008; 4:e1000076. [PubMed: 18497861]
10. Weiner BM, Kleckner N. Cell. 1994; 77:977. [PubMed: 8020104]
11. Hunter, N. Molecular Genetics of Recombination. Aguilera, A.; Rothstein, R., editors. Vol. 17. Springer-Verlag; Heidelberg: 2007. p. 381-442.
12. Storlazzi A, et al. Cell. 2010; 141:94. [PubMed: 20371348]
13. Burgoyne PS, Mahadevaiah SK, Turner JM. Nat Rev Genet. 2009; 10:207. [PubMed: 19188923]
14. Perry J, Palmer S, Gabriel A, Ashworth A. Genome Res. 2001; 11:1826. [PubMed: 11691846]
15. Blat Y, Protacio RU, Hunter N, Kleckner N. Cell. 2002; 111:791. [PubMed: 12526806]
16. Zickler D, Kleckner N. Annu Rev Genet. 1999; 33:603. [PubMed: 10690419]
17. Revenkova E, et al. Nat Cell Biol. 2004; 6:555. [PubMed: 15146193]
18. Kleckner N, Storlazzi A, Zickler D. Trends Genet. 2003; 19:623. [PubMed: 14585614]
19. Froenicke L, Anderson LK, Wienberg J, Ashley T. Am J Hum Genet. 2002; 71:1353. [PubMed: 12432495]
20. Romanienko PJ, Camerini-Otero RD. Genomics. 1999; 61:156. [PubMed: 10534401]
21. Keeney S, et al. Genomics. 1999; 61:170. [PubMed: 10534402]
22. Bellani MA, Boateng KA, McLeod D, Camerini-Otero RD. Mol Cell Biol. 2010; 30:4391. [PubMed: 20647542]
23. Neale MJ, Pan J, Keeney S. Nature. 2005; 436:1053. [PubMed: 16107854]
24. Romanienko, PJ. Ph D dissertation. Cornell University; 1997.
25. Di Giacomo M, et al. Proc Natl Acad Sci U S A. 2005; 102:737. [PubMed: 15640358]
26. Eaker S, Cobb J, Pyle A, Handel MA. Dev Biol. 2002; 249:85. [PubMed: 12217320]
27. Odorisio T, Rodriguez TA, Evans EP, Clarke AR, Burgoyne PS. Nat Genet. 1998; 18:257. [PubMed: 9500548]

28. Hall H, Hunt P, Hassold T. Curr Opin Genet Dev. 2006; 16:323. [PubMed: 16647844]

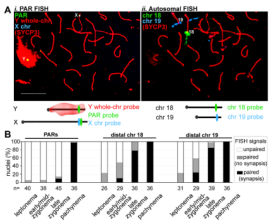

Figure 1.

Late PAR pairing during male meiosis. **A.** FISH assay for pairing. *i–ii*) Example of immunofluorescence (IF) and two sequential rounds of FISH on a late zygotene spermatocyte nucleus. Nuclei stained with an antibody against axis protein SYCP3 were subjected first to PAR FISH (*i*), then to distal-chr18 and distal-chr19 FISH (*ii*). Scale bar, 10 μm. **B.** Nuclei (%) with unpaired and paired (≤2 μm apart) FISH signals. Chromosome synapsis status was also recorded at sites of paired signals.

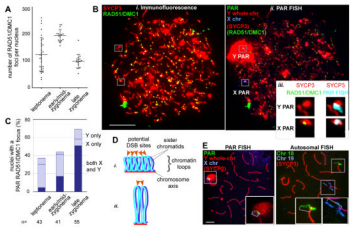

Figure 2.

Distinct temporal and structural properties of the PAR. **A.** Nucleus-wide RAD51/DMC1 foci in spermatocytes (bars = mean±SD). **B.** Assay for PAR DSB formation. IF against RAD51/DMC1 and SYCP3 (*i*) and FISH (*ii*) with probes shown in Figure 1A*i* on a leptotene spermatocyte nucleus. Scale bar, 10 μm. *iii*, Zoom-ins of Y and X PARs from *i* (29), and an overlay of the PAR FISH signal with SYCP3 (left), here with a RAD51/DMC1 focus only on the X PAR. **C.** Nuclei (%) with one or two PAR RAD51/DMC1 foci. **D.** Axis/loop segments as a determinant of DSB potential (after ref. 15). Only one homolog is shown. DNA organized on a longer axis into more and smaller loops (*i*) has more DSB potential than if the same DNA is organized on a shorter axis into fewer and larger loops (*ii*). **E.** Examples of chromatin extension (grey brackets in insets), see also Table 1. Scale bar, 5 μm.

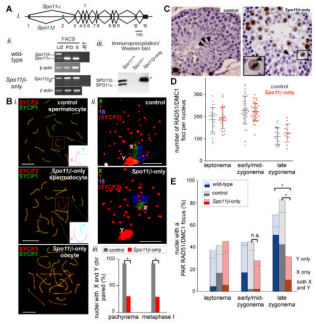

Figure 3.

Genetic control of PAR recombination and pairing. **A.** *Spo11* splice variants (see also fig. S4). *i*) Genomic organization and splicing. *Spo11β* includes exon 2, *Spo11α* excludes it. Y, catalytic tyrosine. *ii–iii*) Reverse transcriptase-PCR from flow-sorted meiocyte populations of adult mice. –RT, no reverse transcriptase; L/Z, leptonema/zygonema; P/D, pachynema/diplonema; S, spermatids. *iv*) SPO11 protein levels in adult testis extracts. Asterisk, a lower-mobility protein likely originating from the knock-out allele (fig. S5D). **B.** IF of SYCP1 and SYCP3 on pachytene nuclei (*i*) and of SYCP3 plus whole-chromosome FISH of early metaphase I spermatocyte nuclei (*ii*) from mice of the indicated genotypes. Inset in (*i*), schematic of X and Y chromosomes. Scale bars, 10 μm. (*iii*) Quantification of X-Y association; 57–65 nuclei scored/genotype. **C.** TUNEL-stained testis sections; apoptotic cells stain brown. Elongating spermatids (arrows) are rare in *Spo11β*-only mice. Inset shows a lagging chromosome (arrowhead) in a TUNEL-positive cell. **D.** RAD51/DMC1 focus counts in spermatocytes from control and *Spo11β*-only mice (bars = mean±SD). **E.** Nuclei (%) with PAR RAD51/DMC1 foci in mice of the indicated genotypes. 41–55 nuclei were scored per stage for each genotype. Asterisks indicate significant differences (P≤ 0.0002, two-tailed Mann-Whitney test). n.s., not significant, P=0.09.

Table 1

Chromosome axis lengths and chromatin extension in PARs and distal ends of Chr 18 and 19.

A. DNA content vs. chromosome axis lengths (late zygonema)

Chromosome	Total size (Mb)	Probe-distal region (Mb)	Total chromosome axis (μm)[a]	Probe-distal axis (μm)[a]	DNA content of probe- distal axis (Mb/μm)
Y	95	0.7	4.2 ± 0.7 (17)	0.7 ± 0.2 (20)	1
X	167	0.7	12.7 ± 2.8 (13)	0.8 ± 0.2 (23)	1
18	91	8	6.1 ± 0.9 (11)	0.6 ± 0.1 (12)	13
19	61	6	5.1 ± 0.5 (11)	0.6 ± 0.1 (10)	10

B. Length of chromatin extension from axes

		FISH signal extension, mean μm ± SD (number of observations)			
Locus	Probe size (kb)[b]	Leptonema	Early/mid-zygonema	Late zygonema	Pachynema
Y PAR	146	0.5 ± 0.2 (25)	0.6 ± 0.3 (21)	0.6 ± 0.3 (21)	1.2 ± 0.5 (23)[c]
X PAR		0.6 ± 0.4 (23)	0.7 ± 0.5 (17)	0.6 ± 0.5 (20)	
Distal Chr 18	207	2.2 ± 0.8 (26)	3.2 ± 1.5 (31)[c]	4.5 ± 1.9 (35)[c]	5.4 ± 2.2 (21)[c]
Distal Chr 19	182	2.3 ± 0.9 (18)	3.6 ± 2.0 (33)[c]	5.3 ± 3.0 (40)[c]	5.9 ± 2.3 (23)[c]

[a] mean ± SD (number of observations)

[b] size of BAC

[c] some or all measurements are from paired FISH signals

Science. Author manuscript; available in PMC 2011 August 5.